DEVELOPMENT OF BLADE PROFILES FOR LOW PRESSURE TURBINE APPLICATIONS

E.M. Curtis, H.P. Hodson, M.R. Banieghbal, J.D.Denton, R.J. Howell
Whittle Laboratory
University of Cambridge
Cambridge, UK

N.W. Harvey
Rolls-Royce plc, Derby, UK

ABSTRACT

This paper describes a programme of work, largely experimental, which was undertaken with the objective of developing an improved blade profile for the low-pressure turbine in aero-engine applications.

Preliminary experiments were conducted using a novel technique. An existing cascade of datum blades was modified to enable the pressure distribution on the suction surface of one of the blades to be altered. Various means, such as shaped inserts, an adjustable flap at the trailing edge, and changing stagger were employed to change the geometry of the passage. These experiments provided boundary layer and lift data for a wide range of suction surface pressure distributions. The data was then used as a guide for the development of new blade profiles. The new blade profiles were then investigated in a low-speed cascade that included a set of moving bars upstream of the cascade of blades to simulate the effect of the incoming wakes from the previous blade row in a multistage turbine environment.

Results are presented for two improved profiles that are compared with a datum representative of current practice. The experimental results include loss measurements by wake traverse, surface pressure distributions, and boundary layer measurements. The cascades were operated over a Reynolds Number range from 0.7×10^5 to 4.0×10^5. The first profile is a "laminar flow" design that was intended to improve the efficiency at the same loading as the datum. The other is a more highly loaded blade profile intended to permit a reduction in blade numbers. The more highly loaded profile is the most promising candidate for inclusion in future designs. It enables blade numbers to be reduced by 20%, without incurring any efficiency penalty. The results also indicate that unsteady effects must be taken into consideration when selecting a blade profile for the low-pressure turbine.

NOMENCLATURE

C_p	Pressure Coefficient (Eq 1)
C_{pb}	Base Pressure Coeff. $\{(p_2-p_b)/(p_{01}-p_2)\}$
D	Diffusion Factor (Eq 2)
o	Throat width
p	Pressure on surface
p_{01}	Stagnation Pressure at Inlet
p_2	Pressure on surface at trailing edge
p_{min}	Minimum pressure on suction surface
R_s	Relative pitch
s	Pitch or Surface length
$s_{bar,}$	Bar spacing
t	Trailing edge thickness
V	Isentropic velocity on surface
V_2	Isentropic velocity on surface at trailing edge
α_2	Outlet flow angle
δ^*	Boundary layer displacement thickness
θ	Boundary layer momentum thickness
ρ	Density
ζ	Loss coefficient (Eq (6))

INTRODUCTION

The low-pressure turbine of a large, high by-pass ratio fan engine provides the power to drive the fan, and often some compressor stages as well. It is constrained to operate at a low rotational speed equal to the fan rpm (unless a gearbox is provided) and this requires several stages, typically about five, and a large diameter. The resulting turbine is heavy, perhaps around one-third of total engine weight, and expensive. The goal of the research programme, part of which is the subject of this paper, was to attempt to improve on the blading currently used in the low-pressure turbine.

There are three factors to take into account in assessing different blade profiles in this context. These are the loss, the weight and the cost.

To be presented at the International Gas Turbine and Aeroengine Congress and Exposition
Birmingham, UK - June 10-13, 1996

In general, the "best" blade will represent the optimum balance between these factors. In this paper, the "cost" of each choice is expressed in terms of bladerow efficiency. To simplify the design problem, all the blade profiles in this programme were designed for the same inlet and outlet flow angles. In other words, they would all have the same stage loading if used in a turbine. Under these circumstances, the blade loading coefficient is directly proportional to the pitch/chord ratio of the bladerow.

The profile for which improvements were sought was a "thin-solid" profile and the other blades developed in the programme were also designed as thin profiles. All profiles were to have the same cross-sectional area as the datum profile and so have the same weight per blade, ignoring any differences in the weight of the shrouds.

The blading in the low-pressure turbine has a large aspect ratio, typically about 5:1. Secondary flows are therefore not a very important feature of the flow. For this reason, the search for improvements concentrated on the blade-to-blade flow and all the experiments were conducted using a rectilinear cascade.

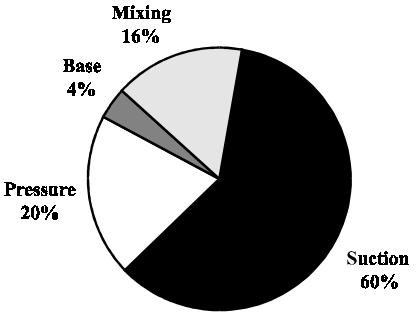

Fig. 1 Estimated Loss Breakdown for Datum Blade

Fig. 1 shows an estimated breakdown of the loss for the datum blade. The data is taken from Banieghbal et al. (1995). The two-dimensional loss is subdivided into four components using the control volume analysis described by Denton (1993). It is evident from fig. 1 that the largest loss arises from the suction side boundary layer. Consequently, the main thrust of the present work was directed at attempting to improve the suction surface flow. The trailing edge is also a significant source of loss and would be improved if trailing edge thickness were reduced or if the shape of the trailing edge were altered. In the work presented here, each profile had the same trailing edge thickness ($\frac{1}{75}$chord) and shape (semicircular). Mechanical integrity prevents the use of very thin trailing edges but an alternative shape such as an elliptical trailing edge may reduce the loss (Sutton, 1990).

At the Reynolds Numbers involved in low-pressure turbines, the flow on the suction surface is likely to remain laminar over a significant fraction of the surface and to undergo transition via a laminar separation bubble shortly after peak suction. Unsteady effects arising from upstream wakes are likely to affect the transition process and the losses. In general the increased turbulence from wakes might be expected to increase losses. A simple theoretical treatment (Hodson et al., 1993) provides a prediction method based on evaluating the increase in boundary layer momentum thickness due to wake-induced transition in attached boundary layers. More recent experimental investigations (Schulte and Hodson, 1994, Banieghbal et al., 1995, Halstead et al., 1995) carried out using hot-film gauges, have indicated that wake effects may be beneficial. This is because they may cause attached laminar-like flow to persist downstream of the nominal separation point, possibly as far back as the trailing edge. Earlier work by Ladwig and Fottner (1993) had shown that stationary wakes could also be beneficial. The results presented here show that the effect of incoming wakes is sometimes to reduce loss, particularly at low Reynolds Number. Schulte and Hodson (1996), who build on the work of Halstead et al. (1995), describe the mechanisms responsible for these observations. The aim of the present paper is to describe a successful strategy for the development of LP profiles with a higher lift than that described by Banieghbal et al. (1995). Hourmouziadis (1989) presented a review of LP turbine aerodynamics that provides a detailed description of the then state-of-the-art.

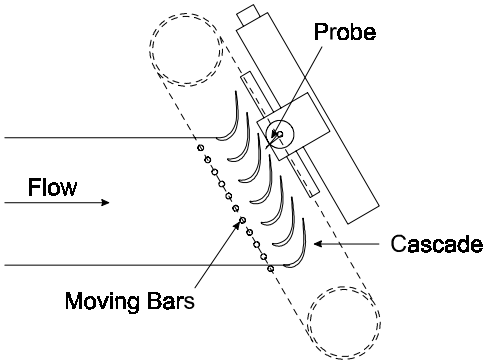

Fig. 2 Schematic Arrangement of Cascade Wind Tunnel

EXPERIMENTAL DETAILS

Datum Cascade

Fig. 2 shows the cascade wind tunnel that was used as the basis for the present investigation. The datum cascade has been described by Banieghbal et al. (1995). It consists of 7 blades, with a chord of approximately 150 mm. The profile of the datum cascade was chosen such that its non-dimensional velocity distribution and exit flow angle matched the normalised Mach number distribution and exit flow angle of the cold-flow turbine investigated by Hodson et al. (1994). Consequently, the air inlet angle is slightly different to that in the cold-flow turbine. Table 1 provides further details of the datum cascade.

To simulate the presence of upstream wakes, and so study the effects of wake-induced transition, the cascade was fitted with a moving bar system (see fig. 2) for some of the later experiments. The bars were driven by a variable-speed DC motor and their speed is continuously monitored during the experiment. The bar speed was set to correspond to a flow coefficient of 0.75. In the actual turbine, the stator blades outnumber the rotor blades. The diameter of the bars (1 mm) and their relative spacing was chosen so as to provide representative wakes during a simulation of the

interaction of stator wakes with a downstream rotor. The bars moved in a plane 0.5 axial chords upstream of the cascade. When the cascade was operated without bars the inlet turbulence was low, approximately 0.5%. Banieghbal et al. (1995) and Schulte and Hodson (1996) provide further details of the facility.

The inlet stagnation temperature was measured using a thermocouple that was placed within the inlet plenum. A Pitot probe placed downstream of the moving bars provided the reference cascade inlet stagnation pressure. By traversing the Pitot in the axial direction in the absence of the cascade, it was shown that the effects of unsteadiness on the readings from this Pitot probe were not significant at the selected measurement location (Schulte and Hodson, 1996).

This cascade had previously been used to measure the losses of the datum blade both with and without the upstream wakes. In the present work it was initially adapted for the 'flap tests' as described in the next section, and later used to measure the losses of the new profiles which were developed, Blades L and H.

Flap Tests

Experiments were undertaken at the start of the current programme to obtain an overview of the potential for designing a blade with an improved suction surface flow, either by reducing the loss or by increasing the loading.

In these experiments only the suction side of the test blade was being investigated. Consequently, there was no requirement to have a periodic cascade. The objective was to determine the suction side loss for a wide range of surface pressure distributions. The variations in surface pressure were achieved by fitting an adjustable flap to the trailing edge of the airfoil adjacent to the one under investigation in the datum cascade. The flap was hinged at the trailing edge of the adjacent blade. Further changes in pressure distribution were made by altering the stagger of the adjacent blade. Fig. 3 shows the arrangement. The hinged flap had a perforated surface and suction could be applied to it using an auxiliary fan in order to prevent the flow separating from the flap at the highest loadings. Inserts to alter the shape of the pressure side of the passage, and splitter vanes, were also used.

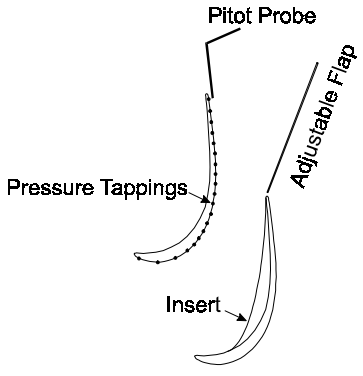

Fig. 3 Typical Arrangement of Flap in Cascade

Blade surface static pressures were determined using pressure tappings located along the midspan section. Boundary layer data were obtained by traversing a flattened Pitot tube, 0.2 mm thick, at a location 1.5 percent of surface length (3 mm) upstream of the trailing edge, adjacent to the final tapping on the suction surface. As the flow is not periodic, data from this final pressure tapping is deemed to be representative of the exit static pressure from the equivalent periodic cascade. For a periodic cascade with Blade H profiles our tests indicated a far-downstream mixed-out velocity head about 3% higher than the dynamic head based on the pressure at the final static tapping. Our definition of diffusion factor is based on the suction surface isentropic velocity since in the 'flap tests' there is no proper cascade outlet condition because the flow is not periodic.

All the data reported here were obtained at a Reynolds number of 2×10^5, based on true chord and exit conditions. The inlet flow was steady with no simulation of incoming wakes for the flap tests conducted using the datum cascade as a basis.

RESULTS AND DISCUSSION

Flap Tests

Velocity Distributions

Blade surface static pressure measurements and their associated boundary layer measurements were made for 42 test cases. The static pressure data are presented in terms of a normalised suction side velocity coefficient defined as

$$\frac{V}{V_2} = \sqrt{C_p} = \sqrt{\frac{P_{01} - p}{P_{01} - p_2}} \qquad (1)$$

Representative velocity distributions are shown in fig. 4. They are identified by the letters A through D. Test cases C and D show that a separation bubble is present, with the bubble occupying approximately 20 percent of the surface length for case C and slightly more for case D. Though not evident in fig. 4, it is likely that the suction side boundary layer will separate in case B. The presence of laminar separation bubbles in at least some of the tests confirms the observations made by Banieghbal et al. (1995) that substantial regions of laminar flow exist under steady flow conditions.

Two parameters that may be significant in defining the velocity distribution are the amount of deceleration from the peak suction point and the location of the peak suction point. The local diffusion factor is defined here as:

$$D = \frac{V_{max}}{V_2} - 1 \qquad (2)$$

The experiments covered a wide range of diffusion factors, from 0.0 to beyond 0.8, and with peak suction position varying from 30% to 85% of surface length. The importance of these parameters is discussed below.

In the flap tests, a pressure distribution is established around a representative airfoil shape. Nevertheless, the actual shape of an airfoil having the same pressure distribution in a periodic cascade would differ. For this reason, it is not possible to determine the

suction side loading by integration of the pressure distribution in the axial direction.

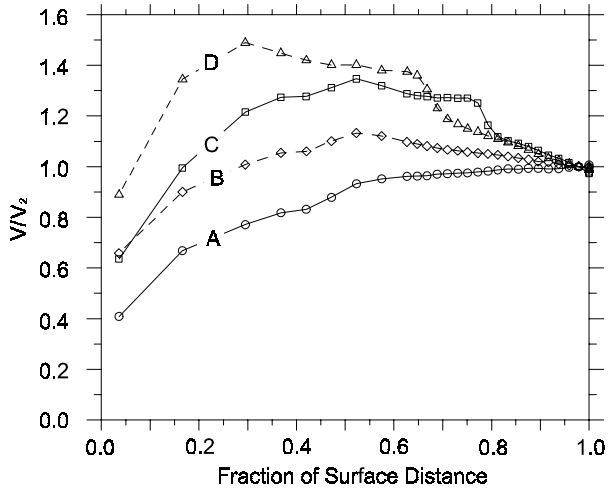

Fig. 4 Typical Flap Test Velocity Distributions

In the present paper, the blade loading is evaluated using the concept of circulation, where

$$\text{Lift} \propto \oint \text{Vds} \tag{3}$$

The flap test experiments give information only about the suction surfaces of alternative designs. To evaluate the circulation and therefore the lift, the contribution of the pressure side is also required. This was assumed to be equal to the value of the integral for the datum blade, as evaluated from the pressure distribution in a periodic cascade experiment. The loading thus evaluated was non-dimensionalised as:

$$\text{Relative Pitch} = R_s = \frac{\int_{\text{Suction}} \text{Vds} - \left(\int_{\text{Pressure}} \text{Vds} \right)_{\text{Datum}}}{\left(\int_{\text{Suction}} \text{Vds} - \int_{\text{Pressure}} \text{Vds} \right)_{\text{Datum}}} \tag{4}$$

The blade numbers corresponding to a particular distribution are inversely proportional to the relative pitch.

Losses

The momentum thickness is plotted against the relative pitch in fig. 5. The maximum value is approximately six times greater than the minimum value whereas the momentum thickness increases ten-fold for the same conditions. Fig. 5 shows that increasing the blade loading will inevitably lead to an increase in the suction side boundary layer thicknesss and that the rate of increase is greater at higher loadings.

From the viewpoint of blading design, the loss data must be set in context. It is to be expected that high suction surface diffusion coefficients will lead to increases in suction surface boundary layer loss. However, in a good design, more diffusion is likely to imply higher loading and therefore a larger pitch. The increased pitch counteracts the increase in boundary layer thickness to some extent. These effects must be taken into consideration when evaluating the suction side loss.

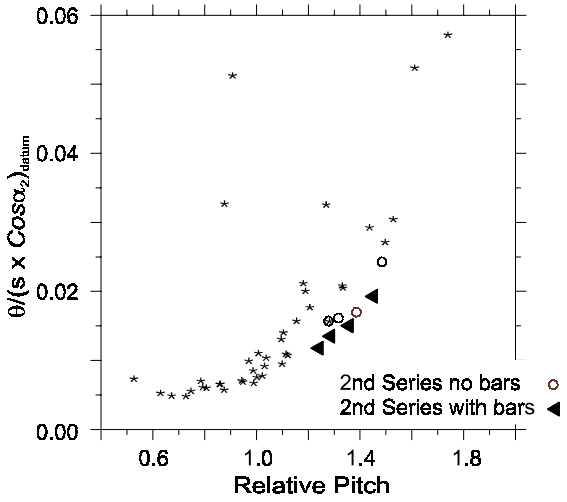

Fig. 5 Flap Tests: Momentum Thickness vs. Relative Pitch

To a first order, the boundary layer momentum thickness at the trailing edge of the suction surface may be represented in the form of a loss coefficient as

$$\frac{2\theta}{R_s \left(s \cos \alpha_2 \right)_{\text{Datum}}} \tag{5}$$

The overall profile loss of any new cascade must include contributions from the pressure side and from the base region of the trailing edge, in addition to the suction side. To relate the momentum thickness measured in the flap tests to the loss for an equivalent blade, a model is required. Here, the expression derived by Denton (1993) for the stagnation pressure loss coefficient using a control volume analysis

$$\varsigma = \frac{\Delta P_0}{0.5 \rho V_2^2} = \frac{C_{pb} t}{o} + \frac{2\theta}{o} + \left(\frac{\delta^* + t}{o} \right)^2$$

where (6)

$$o = R_s \left(s \cos \alpha_2 \right)_{\text{Datum}}$$

is employed to evaluate the overall stagnation pressure loss. The values of boundary layer momentum thickness and displacement thickness are given by the flap tests only for the suction surface and for the pressure surface they are taken as equal to those for the datum blade. In general the pressure surface contribution to the loss is relatively small The base pressure coefficient is difficult to determine. In this case it is assumed to be constant, with a value of 0.1. This is consistent with the application of equation (6) to the datum blade if the loss coefficient ζ is equated to the experimentally determined loss of the datum blade.

Using the assumptions described above and equation (6), it is possible to derive the data plotted in fig. 6. This plot is possibly the most useful for design assessment purposes. The lower edge of the field of points is demarcated by the so-called optimum line.

It indicates the best performance that is to be expected as the loading is varied. The scatter of points above this line is due to the wide range of pressure distributions investigated. Non-optimum distributions would not normally be used for blade design.

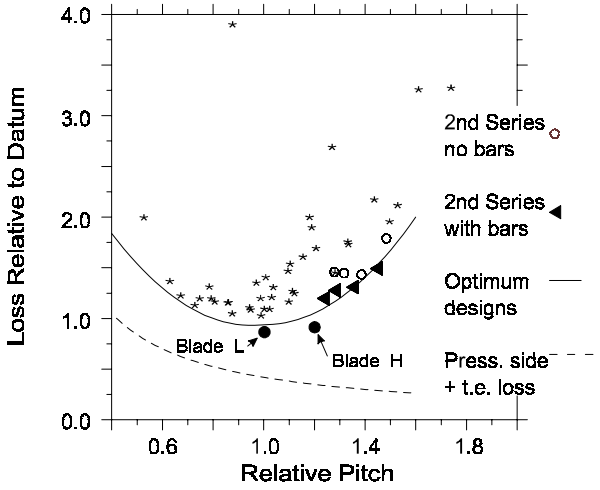

Fig. 6 Flap Tests: Loss vs. Relative Pitch

Fig. 6 shows how, by increasing the pitch (i.e., the loading), the effect of the pressure side and base region losses are diluted. Nevertheless, an important feature of fig. 6 is that the datum blade, with relative pitch of unity, appears to have about the lowest loss. This makes the task of developing a better profile more difficult. Test case B (See fig. 4) lies close to the optimum. It has relatively little suction surface diffusion (D≈0.1).

Test case A has no suction side diffusion. As a consequence, the boundary layer at the trailing edge of the suction surface is laminar. However, the loading is also reduced and the net effect is an increase in profile loss. Thus it would appear that designing for a lower lift than the datum is unattractive since the loss increases and more blades are required.

Test cases C and D have relatively more suction surface diffusion (D≈0.35 and 0.5 respectively) than the datum profile and consequently greater loss. However, the optimum curve is fairly flat around the minimum and a modest increase in lift of, say, 20%, does not result in a large loss increase. Increasing the lift is attractive since, although the loss is likely to increase, weight and cost savings may be achieved.

Fig. 6 gives an optimum based on the flap tests, plus the assumptions on base pressure and pressure side loss. It has the advantage of enabling promising directions for development to be identified. It does not replace the subsequent need to get accurate cascade loss measurements for particular profiles, preferably over a Reynolds Number range and with a simulation of incoming wakes.

Additional Flap Tests

Some additional flap tests were performed recently in order to obtain more complete information relating to the suction surface boundary layer at loadings in the region of 20% to 40% above the datum loading. These used a similar variable geometry arrangement to the original flap tests on a cascade of Blade H profiles. Steady flow and unsteady flow effects were investigated in these additional tests.

The unsteady effects were simulated in these flap tests using moving bars located 90 mm upstream of the leading edge. Relative to the datum cascade, the bar diameter was increased to 2 mm and the spacing of the bars was doubled, in anticipation of operating at higher lift coefficients with higher losses. Schulte and Hodson, (1996) report measurements on the Blade H cascade using the same bars. The boundary layer traverses were obtained with a hot wire probe.

The results from these tests are plotted on fig. 6 along with the original results. The open circles refer to the steady data, the closed triangles to the unsteady data. The results of the additional flap tests, using Blade H, are similar to those of the first series which used the datum blades. It appears, therefore, that the flap test results are not significantly dependent on the precise geometry used to set up the flow. It also shows that the loss is almost the same for the steady and unsteady cases at a Reynolds Number of $2x10^5$ and realistic blade loadings. The latter conclusion is in accordance with the cascade measurements on Blade H described in the next section and is consistent with the view that the unsteady effects due to wakes affect the suction surface loss component and not the trailing edge or pressure side components. It also suggests that the blades of somewhat higher loading than Blade H may have similar suction side boundary layer features.

Diffusion Factors and Loading Distribution

It is often stated that the two parameters that are significant in defining the velocity distribution on the suction surface are the amount of deceleration and the location of the maximum velocity. Lieblein (1956), showed that in the case of compressor airfoils, the loss of a cascade depended only weakly on the (local) diffusion factor as defined by equation (2) until a value of D≈0.4-0.5 was exceeded. Fig. 7 presents selected data from the current flap tests in a form that is similar to that presented by Lieblein. Only those data points that lie closest to the optimum line are shown. Fig. 7 shows that the loss of an 'optimum' cascade is essentially constant for diffusion factors below D=0.2. The data also show that the loss then begins to increase relatively slowly with diffusion factor until D≈0.4-0.5 is exceeded. It is also noted here that a diffusion factor of 0.8 was about the maximum that could be achieved before the flow failed to reattach by the trailing edge. Of course, a different operating Reynolds number might yield different results.

Following the above observations, the authors attempted to determine whether an aft-loaded or a forward loaded profile gave the lower loss. No clear correlation was found, either by correlating against centre of pressure, or against the location of the point of peak velocity. Previous investigations, Hashimoto and Kimura (1984), and Hoheisel et al (1986), have concluded that aft-loading is preferable, although at similar conditions to the 'flap tests' (low inlet turbulence, low Mach Number) there was not much difference. For our additional 'flap tests' (described later), where inlet wakes were present, aft-loading did appear to

give less loss. It may also be preferable from the viewpoint of secondary flow.

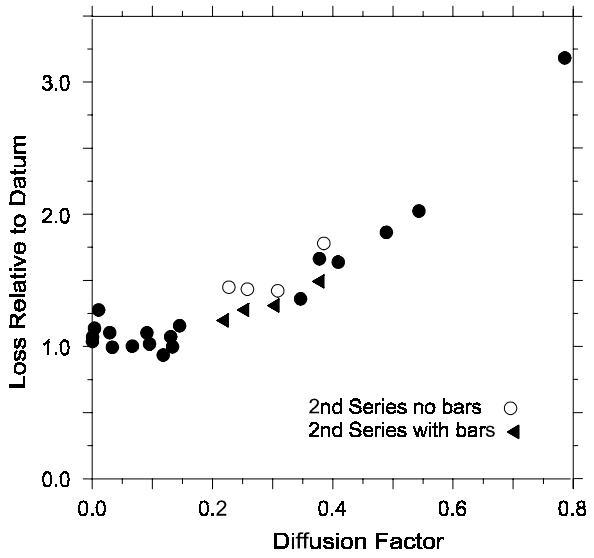

Fig. 7 Flap Tests: Loss vs. Diffusion Factor

Cost Optimisation

Increasing the blade loading reduces the number of blades and, if the weight of an individual blade is not increased, it reduces the overall weight of the engine.

The potential for achieving a benefit in terms of overall costs is illustrated in fig. 8. This is developed from the loss data plotted in fig. 6 and incorporates the cost savings that arise from increasing the pitch and hence reducing the number of blades. This cost saving is due to two factors; the direct saving in manufacturing cost of having fewer blades and the saving on other costs of the associated weight reduction. The cost saving is assumed to be linearly proportional to the pitch.

The parameter Z

$$Z = \frac{\text{Cost saving for 1\% increase in pitch}}{\text{Cost for 1\% point increase in profile loss}} \qquad (7)$$

can be used to denote the exchange rate in terms of cost between a change in pitch and a change in blading loss. It represents the ratio of the cost benefit of a one per cent increase in pitch to the cost resulting from a one per cent point reduction in low-pressure turbine efficiency.

The larger the relative cost benefit of having fewer blades, the larger the value of Z. The curves in fig. 8 show that higher values of pitch are optimum as Z increases. The value of Z to use in a particular case can only be determined by considering all the factors that are relevant. These include the thermodynamic analysis of the cycle, the manufacturing costs, and the application. Fig. 8 is based on losses corresponding to the line drawn on fig. 6 for optimum designs and as the datum blade is somewhat above this line then the minimum of the Z=0 curve in fig. 8 is not located exactly at unity relative pitch or at zero cost difference.

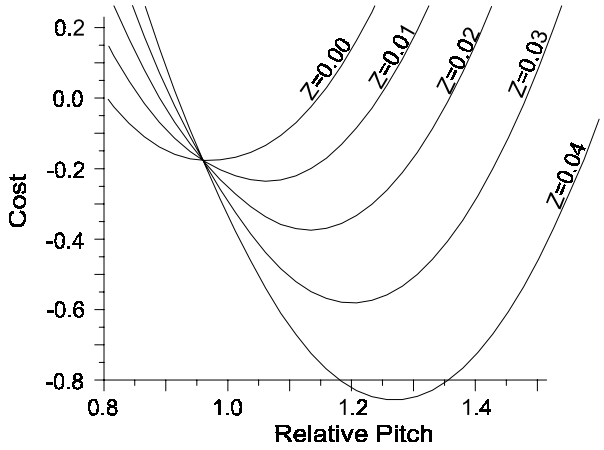

Fig. 8 Flap Tests: Cost vs. Relative Pitch

Cascade Tests

The situation shown in fig. 8 is a useful guide but the underlying assumptions and the limitations of the flap tests mean that some further investigation was required to confirm the performance of particular blade designs. On the basis of the original flap tests it was decided to proceed with the development of two new blade designs and to evaluate their performance in cascade tests. The tests were to be conducted with and without a simulation of incoming wakes. The results were to be compared with the datum blade reported by Banieghbal et al. (1995). Each cascade consisted of seven blades with a nominal chord of 150 mm. Each was tested over a range of Reynolds numbers from 0.7×10^5 up to 4×10^5. The results presented here are for zero incidence.

Pitch-wise traverses were performed at mid-span to measure the profile loss of the three blades at the centre of the cascade. The traverse was performed at a distance 0.25 axial chords downstream of the trailing edge plane of the cascade. A fixed-direction 4-hole Neptune probe was used for these mid-span traverses. The local mean flow angle, static pressure and total pressure were determined from the calibration. Integration of these local values was then carried out using a constant area mixing calculation to provide the required mixed-out values.

A laminar flow design (Blade L)

On the basis of the flap tests the datum blade appears to have a loading close to the optimum for best efficiency. The scope for improving the datum design thus appears limited. However for the datum design the suction side boundary layer undergoes transition via a separation bubble and it seemed there was therefore some possibility of a new design in which suction surface transition was avoided altogether whilst maintaining the same blade loading as the datum blade. Thus the objective for the first of the new designs described here was to have laminar flow on the whole of the suction surface. On the basis that the largest component of loss for the datum blade arises from the momentum thickness of the suction side boundary layer the likely reduction in loss by achieving laminar flow appeared substantial.

The main difficulty with the laminar flow design concept was to achieve sufficient loading when the diffusion had to be limited to a low value to prevent transition from occurring. The curves in fig. 6 and fig. 8 show that the design would be uncompetitive if the loading were reduced much below the datum. For the laminar design, therefore, it was decided to keep the loading at the datum value. The pitch would therefore be the same as for the datum blade and the improvement, if any, would be solely due to a reduction in aerodynamic loss. This blade is referred to in this Paper as Blade L.

An increased lift design (Blade H)

The second new design was intended to have a loading 20% higher than the datum. It was anticipated that it would have a higher loss than the datum blade and would only be competitive if the saving in blade numbers was worth more than the expected reduction in efficiency. The higher loading inevitably involves transition to turbulent flow on the suction surface. The design objectives for this blade were to have a maximum diffusion factor of 0.2 whilst locating the point of maximum velocity as far back as was possible whilst ensuring reattachment of the laminar separation before the trailing edge. It was intended that the extent of the surface covered by turbulent flow would thus be minimised, even though there was no strong evidence to support such a loading distribution from the 'flap tests'. This blade is referred to as Blade H.

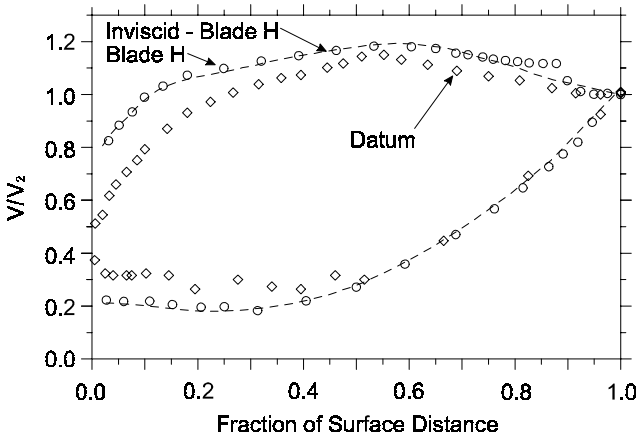

Fig. 9 Velocity Distributions for Datum Blade and Blade H

Velocity Distributions

Plots of isentropic surface velocity distributions are given in fig. 9 for the datum profile, and for the high-lift blade (Blade H). All the data shown here were obtained at a Reynolds number of $2x10^5$.

For the datum cascade, fig. 9 shows maximum velocity occurs at 56 percent surface length, with local diffusion factor D=0.15. Laminar separation is known to occur near 62 percent surface length. On the pressure surface, a separation bubble is again present, the scatter in the data being believed to be associated with unsteadiness in the separation bubble, or with errors in measurement of the low velocities in this region.

The laminar blade (not plotted), has a small amount of diffusion (D≈0.05) and as a consequence, the suction side boundary layer remained attached, (shape factor 2.5, see table 2) at the trailing edge. As compared with the datum blade the loading over the forward part of the blade had to be increased to maintain the loading.

A comparison of the predicted (inviscid) and measured distribution for the high lift blade (fig. 9) reveals a perturbation to the measured distribution that is caused by a laminar separation bubble. Laminar separation occurs at approximately 70 percent surface length and reattachment at about 90 percent of surface length at the design Reynolds number ($2x10^5$). At the lower Reynolds number of $1x10^5$, the pressure distributions showed that reattachment occurs close to the trailing edge. Boundary layer measurements also indicate that the flow remains attached above $Re=1x10^5$. When the incoming wakes are present the observed perturbation of surface pressure by the bubble is reduced and the trailing edge suction surface boundary layers are more turbulent (lower shape factors).

Blade H has a diffusion factor of D=0.20. This is 0.05 greater than the datum cascade and this change, together with an increased loading over the forward part of the blade accounts for the majority of the increase in lift.

The pressure distributions for both Blade L and Blade H are consistent with the design intent for each.

Profile Losses

Table 2 provides a summary of the state and thickness of the trailing edge boundary layers on the three profiles.

Under steady flow conditions, the datum blade has an intermittent attached boundary layer at the trailing edge. For this reason, the shape factor is higher than that of an attached turbulent boundary layer. Under the same circumstances, Blade L has an attached laminar boundary layer at the trailing edge while that for Blade H is attached and turbulent. The loss (i.e. momentum thickness) of the Blade L boundary layer is much reduced by comparison with the datum blade while that for Blade H is much larger. These changes are in line with the design predictions.

With wake-generated unsteadiness at inlet, the datum blade has an almost fully turbulent boundary layer at the trailing edge (Banieghbal et al., 1995). Under the same circumstances, Blade L has an attached transitional boundary layer and Blade H has one that is attached and turbulent. An examination of the momentum thicknesses shows that on the datum blade and Blade L, the losses are increased by the wakes. In both cases, this change is due wake-induced transition. Blade H does not appear to be affected.

Schulte and Hodson (1996) show that the boundary layer on Blade H is also affected by the wakes. While wakes promote transition as they pass over the surface and this serves to increase the loss, the calmed regions that follow these events contain attached laminar flow that persists to the trailing edge. These latter regions produce less loss than would arise in steady flow and so there is little change in the time-averaged loss.

The variations of loss with Reynolds number, for tests without incoming wake disturbances, are plotted in fig. 10. It can be seen

that blades L and H both have a lower loss than the datum blade over most of the Reynolds number range. This is to be expected for Blade L because this has laminar flow over the whole suction surface, but was a surprising result for Blade H.

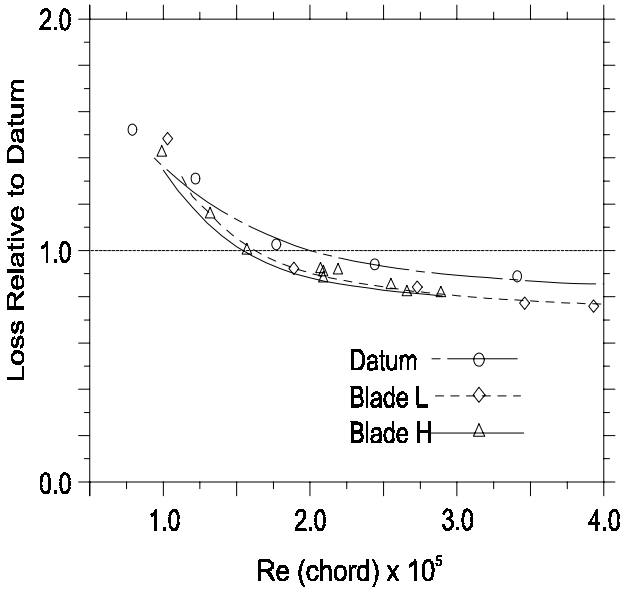

Fig. 10 Cascade Tests: Losses without Bars

Table 3 provides a breakdown of the losses in the manner of equation (6) with and without the wakes. Measured values of boundary layer parameters and of trailing edge pressures are used to derive the tabulated data. Under steady flow conditions, it can be seen that the changes in the boundary layer losses were in line with expectations. Unfortunately, the base pressure loss appears to be higher than that of the datum (attached, intermittent) for Blade L (attached, laminar), and lower than that of the datum for Blade H (attached, turbulent). This suggests that the changes indicated by the changes in boundary layer loss are partially offset by the changes in base pressure. However, it should be noted that estimates of the effect using base pressures from measurements on the cascades showed an effect significantly less than the measured differences in loss as determined from the wake traverses.

The measured cascade losses (steady) for blades L and H have been superimposed on the predictions of fig. 6. Blade L is not directly comparable with flap test predictions because it achieved laminar flow over the entire suction surface whereas the flap tests, at the same loading, did not have laminar flow at the trailing edge, although they did achieve laminar flow at lower loadings. Blade L was expected to have a loss about 75% of the datum loss. The measured loss for Blade L was higher at 88% of datum loss due to the base pressure effect. In contrast the high lift profile, Blade H, benefits from a higher base pressure and so has a lower loss than predicted.

The loss results for the tests with the moving bars at cascade inlet are plotted in fig. 11. As is the case for the tests with no wakes, Blades L and H have lower losses than the datum. For both blades L and H, the gain over the datum is somewhat greater with bars than without. It is also noteworthy that at the lowest Reynolds Numbers, the loss with the bars is smaller than the loss without bars. This is thought to be due to the suppression of separation for the datum blade. In the case of the high lift profile, Blade H, the balance between the increased loss due to wake-induced transition and the reduced loss due to the calmed regions alters. This change is responsible for the improvement (see Schulte and Hodson, 1996).

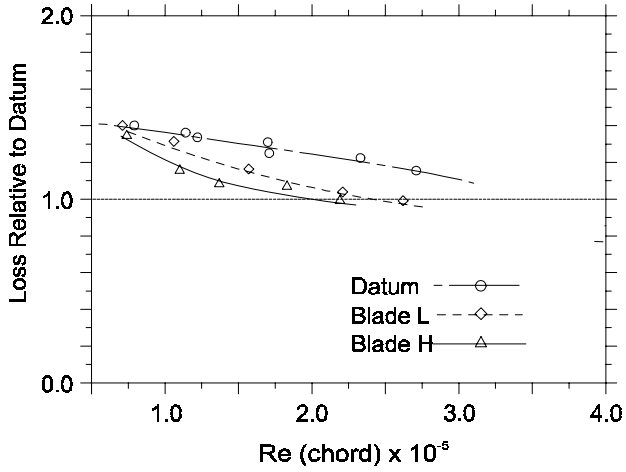

Fig. 11 Cascade Tests: Losses with Bars

In summary, it has been shown that the cascade results show that two effects that were not included in the original flap tests are important. These are the effect of the base pressure and the effect of the wakes. Even though the flap test results differ from the cascade results in detail, they were invaluable in providing wide-ranging data at the start of the profile development process. Finally, it is noted that the profile with the highest efficiency of the three is blade H. Since this also has the highest loading it is the best. The anticipated trade-off between efficiency and loading is not relevant in this particular case.

CONCLUSIONS

1. There is scope for improving LP blade designs by adopting higher loadings than the datum blade.
2. Lower blade loadings than the datum are not attractive.
3. Unsteady effects are important for low-pressure turbine blading and should be simulated in cascade experiments.
4. The unsteady flow features, particularly where transition is involved, mean that CFD cannot yet be relied on for predicting the losses.
5. The loss occurring at the trailing edge is important when comparing different profiles but is difficult to predict.
6. The benefit of a laminar suction surface boundary layer was offset by a high trailing edge loss whereas a more turbulent boundary layer reduced the trailing edge loss.

ACKNOWLEDGEMENT

The authors wish to thank Rolls-Royce plc, and the Defence Research Agency, Pyestock, for their support of the project and their permission to publish this paper.

REFERENCES

Banieghbal, MR, Curtis, EM, Denton, JD, Hodson, HP, Huntsman, I, and Schulte, VS, 1995, "Wake Passing in LP Turbines", Paper No. 23, AGARD conf. Loss Mechanisms and Unsteady Flows in Turbomachines, Derby, May

Denton, J, D, and Cumpsty, N, A, 1987 , "Loss mechanisms in turbomachines", Proc. I. Mech. E., Turbomachinery - Efficiency and Improvement, Paper C260/87, Robinson College, Cambridge, Sept.

Halstead, DE, Wisler, DC, Okiishi, TH, Walker, GJ, Hodson, HP, and Shin, H-W, 1995, "Boundary Layer Development in Axial Compressors and Turbines Part 1 of 4: Composite Picture", ASME Paper No. 95-GT-461, ASME Turbo Expo '95, Houston, Jun.

Halstead, DE, Wisler, DC, Okiishi, TH, Walker, GJ, Hodson, HP, and Shin, H-W, 1995, "Boundary Layer Development in Axial Compressors and Turbines Part 3 of 4: Turbines", ASME Paper No. 95-GT-463, ASME Turbo Expo '95, Houston, Jun.

Hashimoto, K, Kimura, T, 1984, "Preliminary study of forward loaded cascades designed with inverse method for low pressure turbine", ASME 84-GT-65

Hodson, HP, Banieghbal, MR, and Dailey, GM, 1993, "The Analysis and Prediction of the Effects of Bladerow Interactions in Axial Flow Turbines", I Mech. E conf, Turbomachinery, London, Oct. 1994

Hodson, HP, Huntsman, I, and Steele, AB, 1994, "An Investigation of Boundary Layer Development in a Multistage LP Turbine", ASME Jnl. of Turbomachinery, Vol 116, July, pp 375-383

Hoheisel H, Kiock R, Lichtfuss HJ, and Fottner L, 1986, "Influence of free-stream turbulence and blade pressure gradient on boundary layer and loss behaviour of turbine cascades", ASME Paper 86-GT-234

Hourmouziadis, J, 1989, "Aerodynamic Design of Low Pressure Turbines", AGARD Lecture Series LS-167, Jun.

Ladwig, M, Fottner, L, 1993, "Experimental investigations of the influence of incoming wakes on the losses of a linear turbine cascade", ASME 93-GT-394

Lieblein, S, 1956, "Experimental Flow in 2D Cascades", Ch VI of *The Aerodynamic Design of the Axial Flow Compressor*, NACA RME 56B03, reprinted as NASA SP36, 1965.

Schulte, V, and Hodson, HP, 1994, "Wake-Separation Bubble Interaction in Low Pressure Turbines", AIAA-94-2931, AIAA/SAE/ASME/ASEE 30th Joint Propulsion Conference & Exhibit, June

Schulte, V, and Hodson, HP, 1996, "Unsteady Wake-Induced Boundary Layer Transition in Highly Loaded LP Turbines", To be presented at 1996 ASME/IGTI Expo.

Sutton, AJ, 1990, "The Trailing Edge Loss of Subsonic Turbine Blades", Msc Thesis, Univ. Cambridge.

Chord	150 mm
Axial Chord	126.7 mm
Pitch-Chord Ratio	0.68
Aspect Ratio	2.5
Air Inlet Angle (from axial)	30.4°
Design Exit Angle (from axial)	-62.8°
Bar Pitch/Cascade Pitch (1mm bars)	0.667
Bar Passing Frequency (1mm bars)	200 Hz
Axial Distance: Bars-Cascade L.E.	0.5 C_X
Lift Coefficient	0.819
Inlet Free-stream turbulence intensity.	0.5%
Suction Surface Length	193 mm

Table 1 Low speed cascade geometry for datum blade

	Without Bars		With Bars	
	Momentum Thickness (mm)	Shape Factor	Momentum Thickness (mm)	Shape Factor
Datum	0.30	2.4	0.49	1.7
Blade H	0.56	1.6	0.56	1.6
Blade L	0.20	2.5	0.33	2.1

Table 2 Measured Suction Surface Boundary Layer Parameters (Reynolds Number 2 x 10^5, measured 3mm upstream of trailing edge)

Blade	With Bars	Base Pressure Loss	Boundary Layer Loss	Trailing Edge Blockage	Sum of Previous Columns	Measured Loss
		$\frac{-C_{pb}t}{s\cos\alpha_2}$	$\frac{2\theta}{s\cos\alpha_2}$	$\left(\frac{\delta^* + t}{s\cos\alpha_2}\right)^2$	$\frac{\Delta P_0}{P_{02} - p_2}$	$\frac{\Delta P_0}{P_{02} - p_2}$
Datum		0.041	0.878	0.190	1.109	1.0
Datum	√	0.041	1.267	0.190	1.357	1.493
L		0.104	0.557	0.163	0.824	0.878
L	√	0.104	0.787	0.163	1.054	1.109
H		-0.045	1.059	0.154	1.167	0.932
H	√	-0.036	1.077	0.136	1.177	1.054

Table 3 Breakdown of cascade losses relative to datum at Re=2.0x10^5